Hindawi
Advances in Materials Science and Engineering
Volume 2021, Article ID 6637999, 17 pages
https://doi.org/10.1155/2021/6637999

Research Article

Identifying the Thermal Storage Stability of Polymer-Modified Asphalt with Carbon Nanotubes Based on Its Macroperformance and Micromorphology

Xi-yin Liu,[1] **Peng Wang**,[1] **Yu Lu**,[2] **Tian-tao Zhang**,[2] **Li-zhi Wang**,[1] **and Tong-fu Wang**[2]

[1]*School of Transportation Engineering, Shandong Jianzhu University, Jinan, Shandong 250101, China*
[2]*Construction Management Branch, Shandong Hi-Speed Group Co. Ltd., Jinan, Shandong 250101, China*

Correspondence should be addressed to Peng Wang; peng0462@126.com

Received 29 December 2020; Revised 19 February 2021; Accepted 15 March 2021; Published 23 April 2021

Academic Editor: Robert Černý

The thermal storage stability of polymer-modified asphalt (PMA) is the key to avoid performance attenuation during storage and transportation in pavement engineering. However, phase separation of PMA continuously occurs after long-term thermal storage due to the overlooked influence of the phase interface. Two kinds of carbon nanotubes (CNTs) and styrene-butadiene-styrene triblock copolymer (SBS) were selected in this paper to address the aforementioned issue. The segregation test was used to simulate the long-term storage process from 0 to 10 days. Macroperformance included the softening point difference (△SP), irrecoverable compliance (*J*nr), recovery rate (*R*%), and complex modulus (*G*∗) measured by the softening point test, multistress creep recovery (MSCR) test, and small strain oscillatory rheological test. Microcharacteristics were obtained by the SBS characteristic peak index, SBS-rich phase distribution, polymer swelling degree, and particle characteristics of the SBS-rich phase. They were measured by Fourier-transformed infrared spectroscopy (FT-IR), fluorescence microscopy (FM), and atomic force microscopy (AFM), respectively. Results showed that the optimum CNT amount necessary to obtain an improved thermal storage stability of PMA was 0.5 wt.%. After 10 days of storage, the largest *R*% of SBS modified asphalt (SBSMA) decreased to 2.24% and the smallest J_{nr} increased to 0.069 1/kPa, while *R*% of SBSMA with CNTs was 62.15% and its J_{nr} was 0.013 1/kPa. *R*% and J_{nr} of SBSMA with CNTs showed almost no change after 6 days of storage, implying an effective antirutting performance. The results from the micro-performance investigation showed that phase separation of SBS mainly occurred on day 4, while SBS degradation and base asphalt aging led to the worse macroperformance after 10 days of storage. Additional CNTs restrained the SBS-rich phase from floating upward. Meanwhile, a small size of polymer-rich phase and dense network of SBSMA with CNTs were observed in fluorescence microscopy and atomic force microscopy images, thereby exhibiting improved thermal storage stability. Adding CNTs would retard the segregation due to CNT entanglement with SBS.

1. Introduction

Polymer-modified asphalt (PMA) is regarded as the main pavement material due to its excellent performance compared with the traditional one [1]. However, the inevitable high-temperature transportation and storage remain as challenges for PMA. Each asphalt tank truck can load approximately 40 tons of asphalt. Using up a truck of asphalt in a short time is difficult, especially during bad weather in pavement engineering. Therefore, PMA must be stored around 160°C in the asphalt mixing station for a long time [2].

The performance degradation of PMA is inevitable during transportation and storage due to poor thermal storage stability [3]. The most popular polymer modifier is styrene-butadiene-styrene triblock copolymer (SBS), and its marketing share has exceeded 90% worldwide. Thus, we take the SBS modified asphalt (SBSMA) as an example in this paper. The SBSMA is essentially a thermodynamically incompatible system [4]. At high temperatures, the small particle of SBS is automatically aggregated into the large size and separated from the asphalt phase, thereby causing SBS phase agglomeration and floating on the surface of the

asphalt matrix [5]. Finally, the SBSMA performance is deteriorated due to the phase separation of SBS and asphalt [6]. The thermal storage stability of polymer-modified asphalt captures the performance change during high-temperature conditions. Therefore, this performance has been getting a lot of attention.

Many methods are used to improve the thermal storage stability of SBSMA. Mouillet et al. reported that gravity is the direct cause of phase separation [7]. Thus, changing the density difference between SBS and asphalt would improve the thermal storage stability. Wang et al. indicated that adding aromatic oil would help obtain effective compatibility of asphalt and SBS because aromatic compounds in asphalt had a strong interaction with polybutadiene in SBS [8]. However, Sun and Lu studied and interpreted the different hot storage stabilities of three SBS modified asphalts with the interface layer principle; the results show that physical modification methods cannot work because SBS interphase still relied on van der Waals forces to form the physical network [9]. Lesueur reported that the physical network of SBS would be destroyed by heating or adding external force, thereby leading to the agglomeration and separation of the SBS-rich phase from the asphalt phase [10]. Thus, some chemical methods were proposed. The most widely used method is the sulfur crosslinking agent. However, Zhu et al. revealed that sulfur cross-linked SBS modified asphalt was sensitive to oxygen and easily leads to aging and bond breaking [11]. The thermal separation of SBSMA remains unsolved if only the sulfur crosslinking agent is used. Wang et al. demonstrated that the weak interphase between SBS and asphalt resulted in poor thermal storage stability based on polyphase material mechanics and with the help of the Palierne model [12]. Zhu et al. established a PMB phase field model considering viscoelasticity and calibrated it with the experimental observations of three different PMBs; they reported that the separation of SBSMA was subjected to interphase characteristics [13]. Carbon nanotubes (CNTs) were used to improve the interphase strength of composite and increase asphalt performance [14, 15]. However, the effect of different kinds of CNTs on the long-term thermal storage stability of SBSMA was unclear.

This paper aims to investigate the improvement of thermal storage stability for SBSMA with or without CNTs. Multiwalled CNTs were selected, and two ways of adding CNTs in the asphalt were proposed. The segregation test was used to simulate the thermal storage procedure. Macroperformance was obtained from the softening point test, multistress creep recovery test, and small strain oscillatory rheological test. Microcharacteristic indexes were captured by FT-IR, FM, and AFM. Here, microcharacteristics were used to elucidate the thermal storage performance changes with time, including SBS characteristics peak index, SBS-rich phase distribution and swelling degree, and SBS-rich phase particle characteristics. The work would provide some new ideas to identify the polymer-rich phase segregation of polymer-modified asphalt completely.

2. Materials and Methods

2.1. Materials. The raw material included straight asphalt, SBS polymer, CNTs, and stabilizer. Straight asphalt with penetration of 70 dmm was used as base asphalt (marked as A70#); the technical properties are shown in Table 1. Linear type SBS with molecular weight of 110000 g/mol was used in this research, and the block ratio of styrene to butadiene is 3 : 7. CNTs were surface-modified with hydroxyl. Stabilizer was a type of commercial sulfur crosslinking agent. It is composed of 80% sulfur powder and 20% filler, in which the filler is nano calcium carbonate.

Two types of CNTs were selected, marked as CNTs-I and CNTs-II, respectively, as seen in Figure 1, and the technical properties are shown in Table 2. CNTs-I are the original multiwalled carbon nanotubes with hydroxyl, the length of CNTs is 10–30 μm, and the relative content of functional groups is 2.1 mmol/g. CNTs-II refer to the SBS polymer alloy with original multiwalled carbon nanotubes containing hydroxyl.

2.2. Preparation of Polymer-Modified Asphalt Samples. Polymer-modified asphalt samples were prepared using a high-shear mixer (WeiYu Machine Co., Ltd, Shanghai, China). Base asphalt was heated at 160°C for improved flow. SBS and CNTs were added to the mixture of asphalt at 180°C for 30 min at a fixed rotation speed for 3000–3500 r/min. Thereafter, asphalt stabilizer (0.25 wt.% by asphalt weight) was added into the mixtures at 175°C for 5 min at a fixed rotation speed of 2500 r/min. Finally, the mixture temperature was decreased to allow the polymer swelling and prevent asphalt aging.

Moreover, CNTs-I and CNTs-II showed similar adding methods into the asphalt. However, CNTs-I were blended with SBS particle in advance, while CNTs-II were directly added into the heated base asphalt mixed with SBS particle. The obtained asphalt was marked as SBSMA, SBS + CNTs-I, and SBS + CNTs-II. Herein, SBSMA referred to polymer-modified asphalt only using SBS particle, SBS + CNTs-I contained SBS particle and CNTs-I, and SBS + CNTs-II contained SBS and CNTs-II. All polymer-modified asphalts satisfied the relevant requirements of I-C grade modified asphalt according to the "Technical Specification for Highway Asphalt Pavement Construction" (F40-2004) in China. The samples used in the test are shown in Table 3.

2.3. Experimental Methods. The storage samples used in the test were obtained from the segregation test in accordance with ASTM D 5975. The process of segregation test is shown in Figure 2. However, the storage time was not only 48 h. In the CNTs content determination part, the segregation time was 48 h. The SBS + CNTs-I samples were prepared for testing with 0 wt.%, 0.2 wt.%, 0.5 wt.%, and 1 wt.% of CNTs-I combined with a solid 4.0 wt.% SBS by weight of asphalt. Meanwhile, the SBS + CNTs-II samples were prepared for testing with 0 wt.%, 0.5 wt.%, 1.5 wt.%, and 2.5 wt.% of

Table 1: Technical characteristics of A70# asphalt binders.

	Index	Test result	Technical requirement
	25°C, 100 g, 5s, penetration (0.1 mm)	63	60~80
	Penetration index	−1.45	−1.5~+1.0
	Softening point (°C)	46.2	<46
	60°C, dynamic viscosity (Pa.s)	248	<180
	10°C, 5 cm/min, ductility (cm)	22.51	<20
	Wax content (%)	2.18	<2.2
	Quality change (%)	0.05	> ± 0.8
RTFOT	25°C, residual penetration ratio (%)	73.85	<61
	10°C, residual ductility (cm)	9	<6

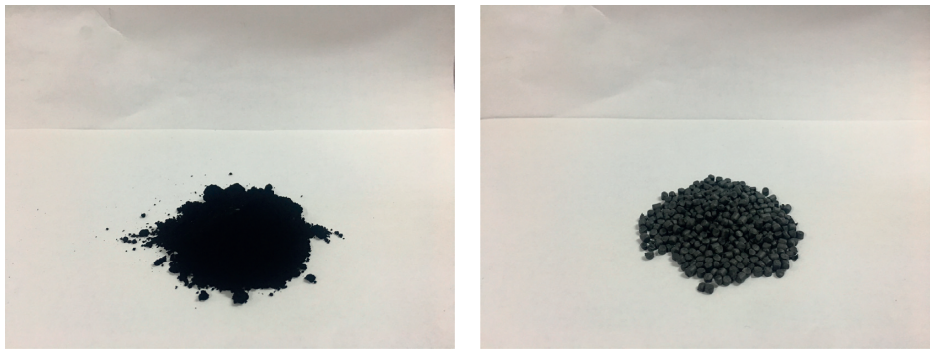

(a) (b)

Figure 1: CNTs used in the test. (a) CNTs-I. (b) CNTs-II.

Table 2: Key technical characteristic parameters of SBS polymer and CNTs.

Linear SBS		Multiwalled CNTs	
Polybutadiene content (%)	70	External diameter (nm)	30~50
Polystyrene content (%)	30	Length (μm)	10~30
Molecular weight ($g \times mol^{-1}$)	110000	Bulk density ($g \times cm^{-3}$)	0.09

Table 3: Samples used in the test.

Sample	SBS content (wt.%)	CNTs content (wt.%)
SBSMA	4.0	0
SBS + CNTs-I PMA	4.0	0/0.2/0.5/1.0
SBS + CNTs-II PMA	4.0	0/0.5/1.5/2.5

CNTs-II combined with a total of 4.0 wt.% SBS by weight of asphalt. The effective CNTs in CNTs-II were the same as those in CNTs-I. Thus, the amount of CNTs-II was similar to CNTs-I in subsequent sections. The experimental design flowchart is shown in Figure 3.

The macroperformance of SBSMA was obtained by the softening point test, multistress creep recovery (MSCR) test, and small strain oscillatory rheological test. The softening point difference (△SP) was obtained by measuring the softening point at the top and bottom of the sample by the global method in accordance with ASTM D5976. MSCR was used to capture irrecoverable compliance (J_{nr}), recovery rate(R%), and accumulative strain in accordance with ASTM D7405-10a. The small strain oscillatory rheological test was used to get the complex modulus ($G*$) on the dynamic shear rheometer (DSR) with a temperature at 70°C. MSCR and small strain oscillatory rheological tests are carried out on the dynamic shear rheometer (DSR). The test principle is that the rotation axis applies periodic sinusoidal shear stress to the asphalt sample, from point A to point B, then back to point A, then to point C, and finally back to point A, which is completed in one cycle, as shown in Figure 4.

The microscopy tests were conducted using FT-IR, FM, and AFM. FT-IR was used to capture the SBS characteristic peaks changes, which was performed on TENSOR II in the storage process of SBSMA, the number of tracing is 64 cm^{-1}, and the resolution is 4 cm^{-1}. FM was used to observe the SBS-rich phase distribution, and AFM was used to identify the particle characteristics of SBS-rich phase. FM was conducted on Leica DM 2500, and the magnification is 100x. AFM was performed by the Bruker Dimension Fast Scan, and the sample test range is 50 $\mu m \times 50\ \mu m$, 10 $\mu m \times 10\ \mu m$, and 3 $\mu m \times 3\ \mu m$. The scanning frequency is 1 Hz, and the scanning resolution is 256 frames × 256 frames. Digital image technology was used to find the SBS swelling degree and particle characteristic indexes. The asphalt films for FM and AFM were obtained by employing a heat-casted method. A hot asphalt binder was cast into glass slides to achieve effective flow with a heating temperature of approximately 160°C. Bitumen-covered sample holders were left overnight at room temperature before testing.

In addition, the degree of separation (△ parameters) was used to capture the performance differences between the top

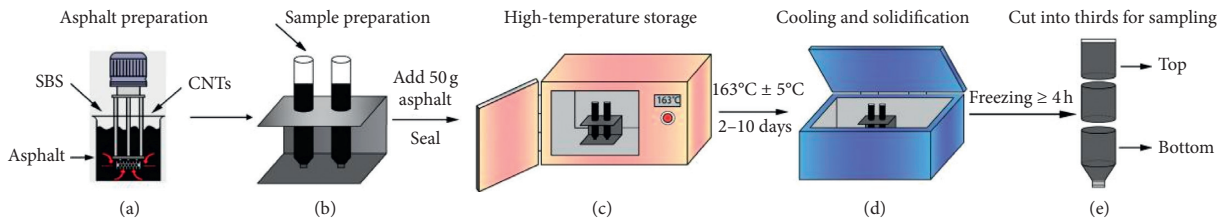

Figure 2: Segregation test of polymer-modified asphalt.

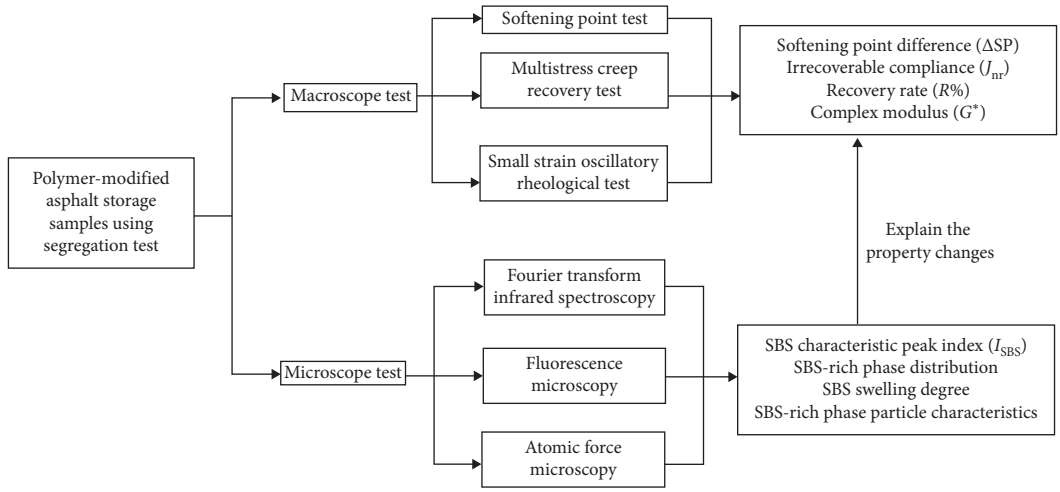

Figure 3: Experimental design flowchart.

and bottom of the sample during storage, as seen in equation (1). The parameters can be modulus, SBS characteristic peak index, etc.

$$\text{Degree of separation } (\Delta \text{ parameters}) = \left| \frac{\text{top parameters} - \text{bottom parameters}}{\text{average of the top and bottom parameters}} \right| \times 100\%. \quad (1)$$

3. Results and Discussion

3.1. Determination of CNT Amount in SBSMA. CNT amount plays a crucial role on the thermal storage property of SBSMA. The standard segregation test was used to obtain the 48 h storage asphalt samples with different CNT amounts. The conventional index (△SP) and rheological indexes (R%, J_{nr}, and $G*$) were used to identify the thermal storage stability changes of SBSMA with CNT amount during storage procedure.

△SP was a common index used to evaluate the segregation degree and the performance deterioration of PMA. A large △SP demonstrated poor thermal storage stability. In Figure 5, the samples with CNTs all satisfied the requirement of specification in China. For the sample of SBS + CNTs-I, △SP decreased at first and then increased, yet the smallest △SP was observed at 0.5 wt.%. This phenomenon was ascribed to the addition of appropriate amount of CNTs can improve the stability of SBSMA, but the accumulation of a large number of CNTs in asphalt will lose the reinforcement capability of asphalt. For the sample of SBS + CNTs-II, △SP decreased with CNTs-II amount. No peak was observed in the curves of △SP in Figure 5(b). However, another study pointed out that this conventional index cannot express segregation accurately [4]. Thus, additional investigations are necessary to find the optimum dosage of CNTs-II in SBSMA.

The MSCR test was selected to identify R and J_{nr} changes with increasing CNT amount, and △R and △J_{nr} were, respectively, calculated from equation (1), as indicated in the results in Figure 6. For the sample of SBS + CNTs-I, Figures 6(a) and 6(b) revealed that R% at the top initially increased and then later decreased, while the value of R% at the bottom initially decreased and then increased. J_{nr} of SBS + CNTs-I presented a similar rule to R%. For the sample of SBS + CNTs-II, the rule of R% was unclear, but the largest R% and the smallest J_{nr} were obtained at the additional 0.5 wt.% CNTs-II. A large R and small J_{nr} revealed a remarkable

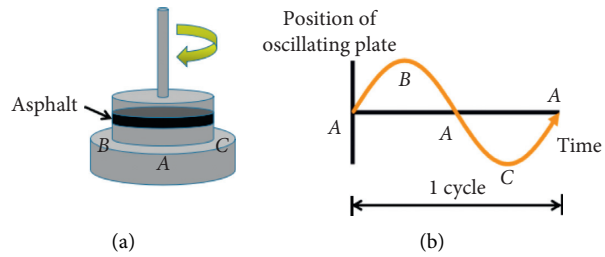

Figure 4: Configuration and load cycle of dynamic shear rheometer.

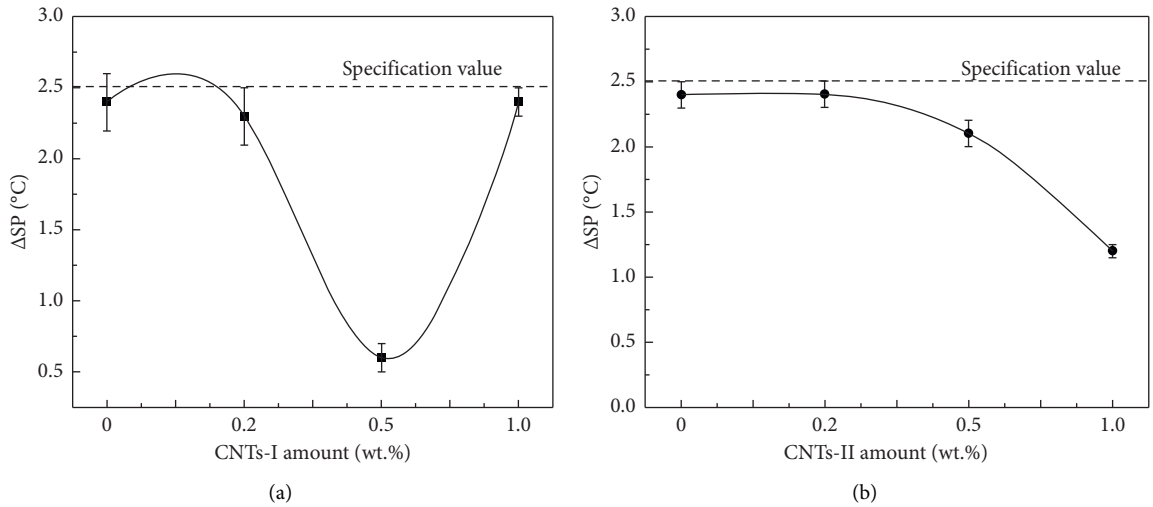

Figure 5: Effect of different amounts of CNTs on △SP after 2 days of segregation. (a) △SP changes of CNTs-I. (b) △SP changes of CNTs-II.

antirutting performance of PMA [10]. Thus, additional 0.5 wt.% CNTs would help obtain effective high-temperature performance. Meanwhile, the results in Figures 6(c) and 6(d) showed that $\triangle R$ decreased before CNTs were below 0.5 wt.% and increased when CNTs surpassed 0.5 wt.%. For the addition of 0.2 wt.% CNTs, $\triangle R$ of SBSMA with CNTs-I was larger than that with CNTs-II, while the rule of $\triangle J_{nr}$ was completely opposite. The value of $\triangle J_{nr}$ for SBS + CNTs-I initially decreased and then increased. By contrast, the value for additional CNTs-II initially increased and then decreased, thereby finally raising the CNT amount. This phenomenon might be subject to the discrepancy in the interaction between CNTs and SBS among the asphalt matrix. The small $\triangle R$ and $\triangle J_{nr}$ illustrated a minimal difference between the top and bottom of SBSMA during the storage process. Thus, the optimum amount of CNTs was 0.5 wt.% from the high-temperature performance of SBSMA (Figure 2).

Figure 7 provides the complex modulus ($G*$) variation of SBSMA with different types of CNTs. For SBS + CNTs-I, $G*$ significantly decreased with CNTs-I amount at the top of asphalt samples in Figure 7(a). By contrast, $G*$ initially decreased but later increased at the bottom with increasing CNTs-I amount. For SBS + CNTs-II, $G*$ at the top slightly decreased, while the value of $G*$ at the bottom almost remained constant with increasing CNTs-II amount. Compared with CNTs-I and CNTs-II, the samples with 0.2 wt.% CNTs-II at the top had the smallest modulus, while the one with 1.0 wt.% CNTs-I at the bottom had the largest modulus. A large modulus would provide improved high-temperature strength [6]. Thus, the modulus changes in asphalt indicated that the top and bottom of SBSMA had different high-temperature deformation resistance. Figure 7(b) revealed that $\triangle G*$ initially decreased and then increased with rising CNTs-I amount, while the one with CNTs-II was different. However, the smallest $\triangle G*$ was found in the amount at 0.5 wt.% for both types of CNTs.

Overall, the data of △SP, $\triangle R$, $\triangle$Jnr, and $\triangle G*$ for SBSMA with different types of CNTs had different rules for the thermal storage process. However, the smallest change between the top and bottom for those indexes was an additional 0.5 wt.% CNTs. Thus, the optimum percentage for adding CNTs into SBSMA was 0.5 wt.% for further study.

3.2. Effect of CNTs on the Macroperformance of SBSMA

3.2.1. Difference in Softening Point. Figure 8 shows the rule of △SP changes with increasing storage time. With the extension of storage time ranging from 0 to 10 days, △SP of the three modified asphalts initially increased and then

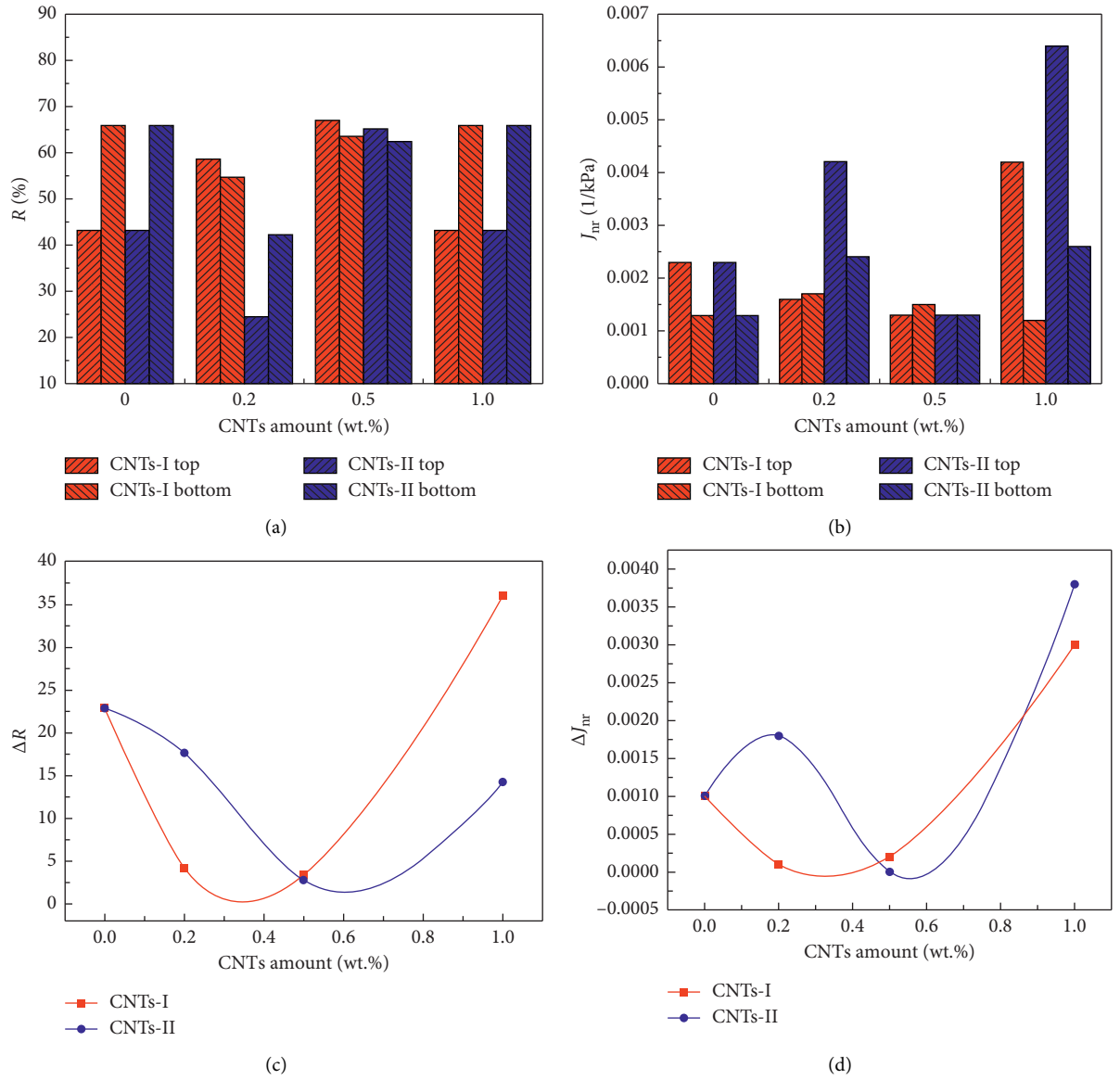

Figure 6: Effect of different amounts of CNTs on R, J_{nr}, $\triangle R$, and $\triangle$Jnr after 2 days of segregation: (a) R, (b) J_{nr}, (c) ΔR, and (d) $\triangle$Jnr for different amounts of CNTs.

decreased. Although SBSMA satisfied the requirement of specification on the 2nd day, the value of $\triangle$SP on the 4th day was beyond this requirement. This trend was ascribed to SBS-rich phase distribution characteristics, base asphalt aging, and SBS degradation in high-temperature conditions [16]. All these factors led to poor network strength of SBS. However, modifying this essential characteristic of the thermodynamic incompatible system is difficult. Comparatively, adding CNTs would improve the degree of deterioration. The SBS + CNTs-I showed more gentle differences of $\triangle$SP than that of neat SBS. Meanwhile, the maximum value of $\triangle$SP for SBS + CNTs-I decreased, thereby demonstrating that adding CNTs-I could decrease the segregation degree of SBSMA. The SBS + CNTs-II had no significant advantage in decreasing $\triangle$SP of SBSMA possibly due to the large cohesive interaction between CNTs and SBS in CNTs-II. However, additional work proved that $\triangle$SP was an ineffective index to evaluate the segregation degree [4]. Thus, the creep characteristics and rheological performance were used for further research.

3.2.2. Creep Characteristics from MSCR Test. R, Jnr, and accumulated strain of three modified asphalt were selected to capture the creep characteristic differences of SBSMA before and after adding two types of CNTs at long-term thermal storage period, as shown in Figures 9 and 10.

Figure 9 shows that the values of R% for SBSMA either in the top or bottom decreased with increasing storage time. The R% value of SBSMA was close to zero after 10 days of thermal storage. The values of J_{nr} for SBSMA increased with storage time. The samples with additional CNTs showed a larger R% and smaller J_{nr} than that without CNTs. A large R% represented that asphalt performed small permanent deformation

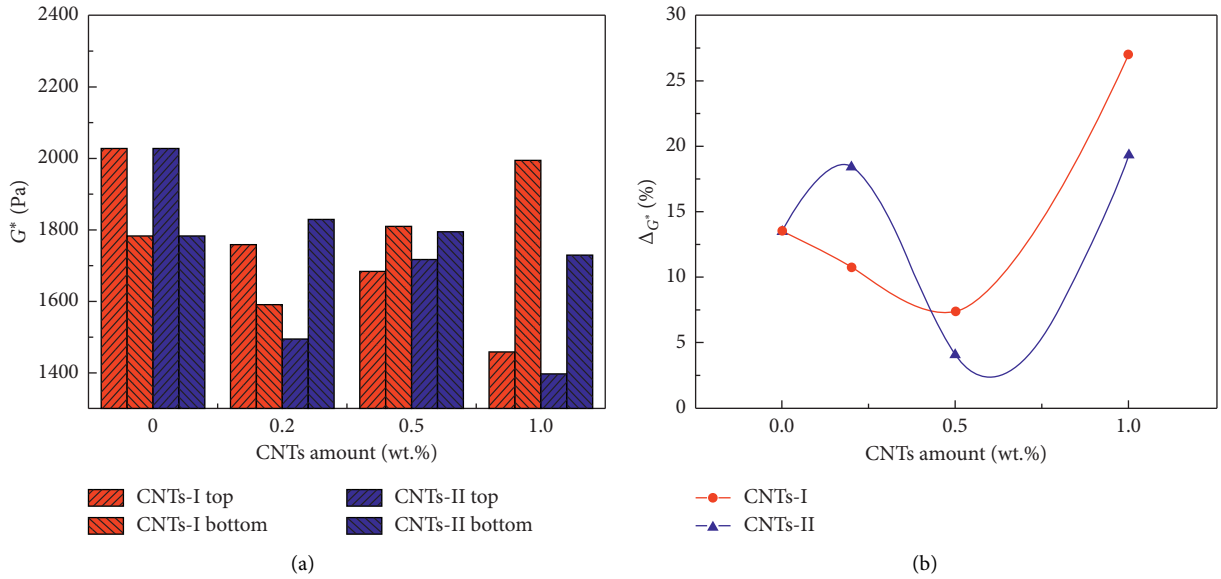

Figure 7: Changes in complex modulus ($G*$) and separation degree ($\triangle G*$) with different CNTs amounts. (a) $G*$ changes with CNTs amounts. (b) $\triangle G*$ changes with CNTs amounts.

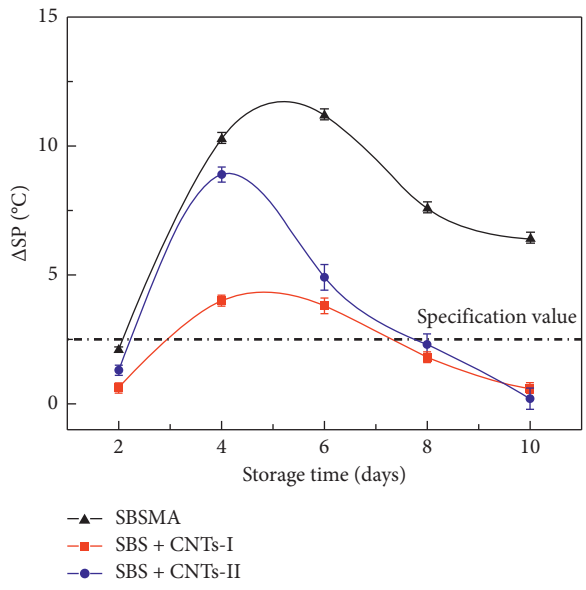

Figure 8: Difference in softening point after separation of three modified asphalts.

caused by the viscous flow and showed low risks of rutting in asphalt pavement [17]. A small J_{nr} means that the asphalt had minimal irrecoverable residual strain and produced small rutting depth in asphalt pavement [17]. Thus, the results in Figure 9 illustrated that additional CNTs could improve the antirutting performance of SBSMA regardless of the CNTs type. Meanwhile, $R\%$ and J_{nr} of the samples with additional CNTs were almost maintained when the time was less than 8 days. This phenomenon demonstrated that additional CNTs could prolong the thermal storage stability to 8 days. Comparing the CNTs-I and CNTs-II, the storage time was less than or equal to 6 days, and the improvement effect of thermal storage stability was similar. Meanwhile, the CNTs-II had better antirutting performances than those with CNTs-I when storage time was higher than 6 days.

Figure 10 shows the accumulative strain of three modified asphalts after 10 days of thermal storage. Either at the top or bottom, the SBSMA showed the largest accumulative strain, the SBS + CNTs-II had the smallest accumulative strain, and the SBS + CNTs-I was between the two. This finding might be ascribed to the distribution of the SBS-rich phase and SBS amount changes in the top and bottom of the asphalt matrix. Combined with the data in Figure 9, neat SBSMA lost its elastic recovery capability after 10 days of storage. Adding CNTs-I into SBSMA, the accumulative strain was reduced, the elastic recovery capability was improved, and the elastic recovery capability of the top and bottom parts had minimal difference. Adding CNTs-II into SBSMA, the accumulative strain of the top was reduced to approximately 1/2 of that of SBSMA, and the value of the bottom reached 1/5 of that of SBSMA. Thus, the results in Figures 9 and 10 revealed that additional CNTs would endow the SBSMA with outstanding elastic recovery capability even after 10 days of thermal storage, and the CNTs-II showed better improvement than that with additional CNTs-I.

3.2.3. Rheological Characteristics from DSR. Complex modulus ($G*$) is an important rheological index, which is closely related to high-temperature performance calculated from the stress-strain ratio of viscoelastic materials subjected to sinusoidal loading. Thus, $G*$ was selected to investigate the rheological characteristics of three modified asphalts, as shown in Figure 11.

Figure 11 provides the $G*$ changes of three modified asphalts with increasing storage time. For SBSMA, $G*$ at the top and bottom substantially decreased with increasing

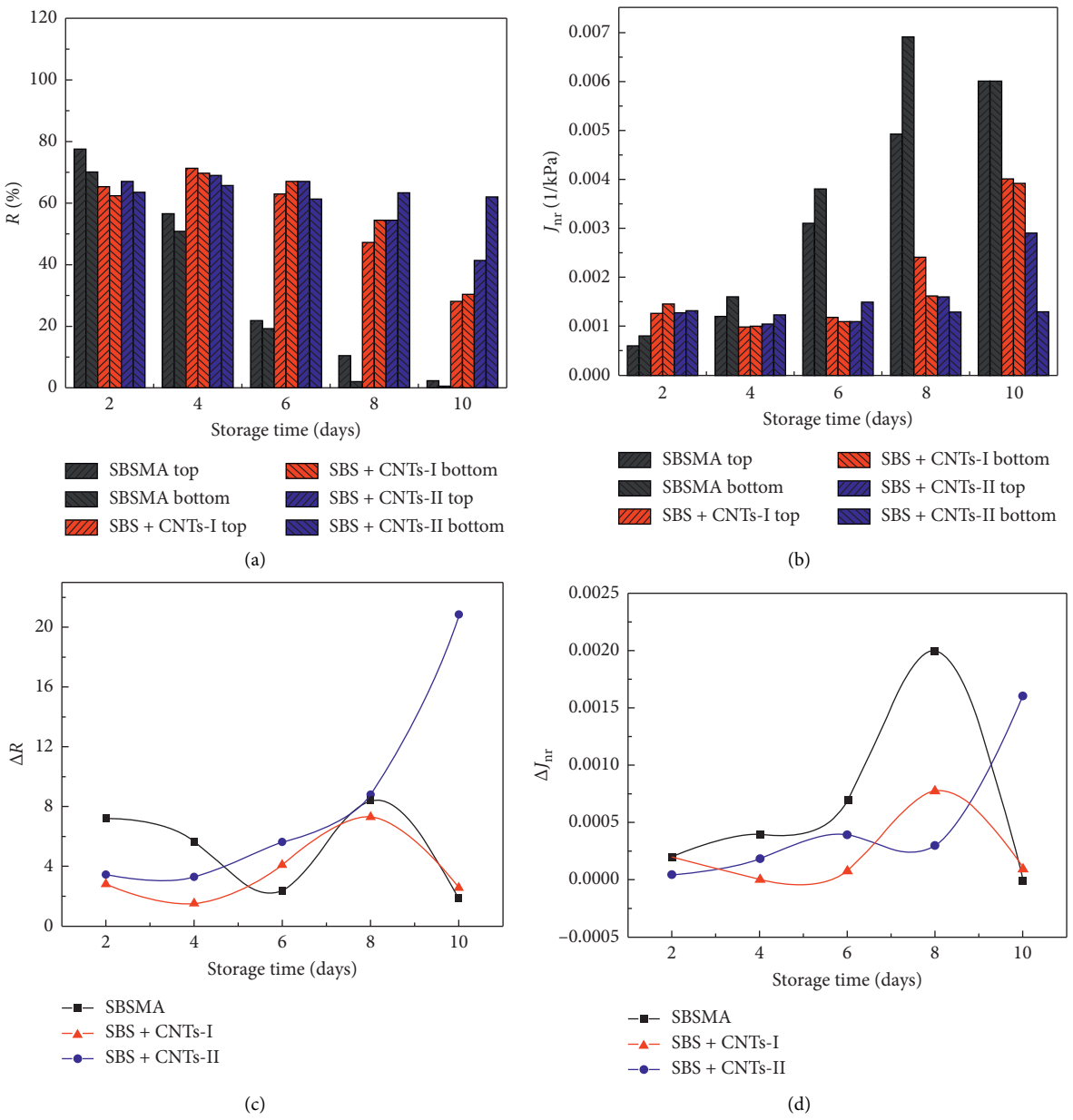

FIGURE 9: R, J_{nr}, ΔR, and $\triangle Jnr$ of three kinds of modified asphalt with different storage times. (a) R, (b) J_{nr}, (c) ΔR, and (d) $\triangle Jnr$ for different storage times.

storage time. $\triangle G*$ on the 2nd day of SBSMA was also larger than that with CNTs. The attenuation rate for the sample of SBSMA containing CNTs was significantly slower than that of SBSMA without CNTs. Compared with the SBS + CNTs-I and SBS + CNTs-II, additional CNTs-I into SBSMA could remarkably minimize the decreasing $G*$ at the top if storage time surpasses 6 days, while $G*$ at the bottom was increasing if the storage time is beyond 2 days. Additional CNTs-II into SBSMA showed similar rules, yet the change degree was not the same in Figure 11(a). This phenomenon demonstrated that the reinforcement of CNTs improved the modulus changes with the degradation of the SBS network in asphalt. Moreover, the modulus was slightly decreased when the storage time surpassed 8 days. This phenomenon illustrates that additional CNTs could slow down the decay of $G*$ during long-term thermal storage and provide improved high-temperature performance. Meanwhile, the CNTs-II showed better improvement than CNTs-I in SBSMA.

3.3. Effect of CNTs on the Microcharacteristics of SBSMA

3.3.1. SBS Characteristic Peak Index Changes from FT-IR. Characteristic peaks in the FT-IR spectrum provided the functional group composition in the substance. Figure 12 summarizes the FT-IR spectra of the three modified asphalt samples with different storage times.

The peaks are divided into two sections in the FT-IR spectra: functional group area (1000–4,000 cm^{-1}) and

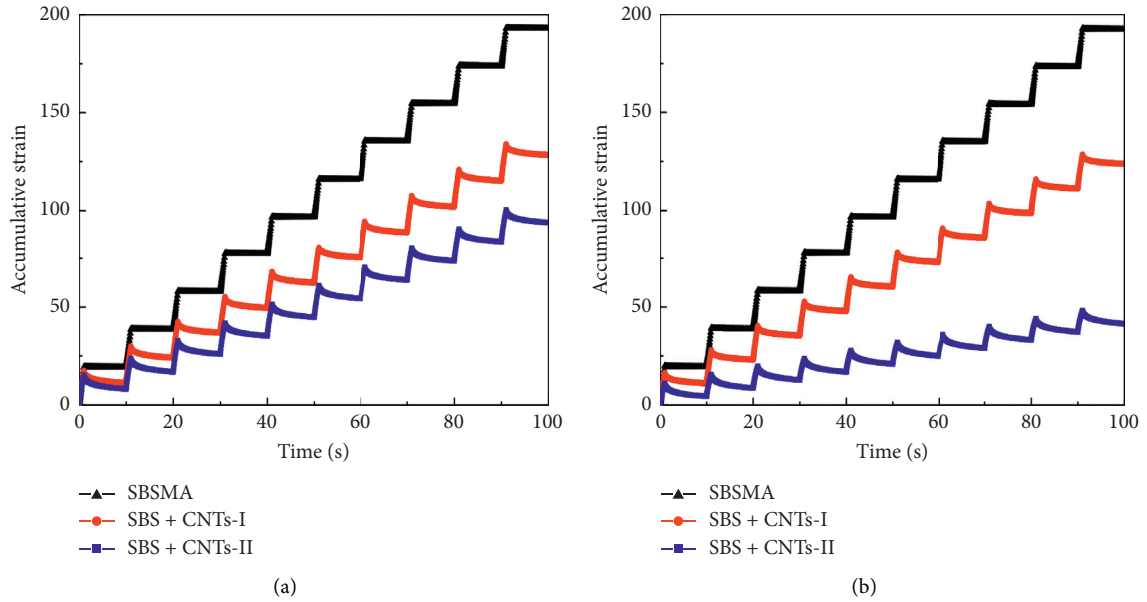

FIGURE 10: Accumulative strain at 3200 Pa of the three modified asphalts stored on the 10th day. (a) The rules of asphalt samples at the top. (b) The rules of asphalt samples at the bottom.

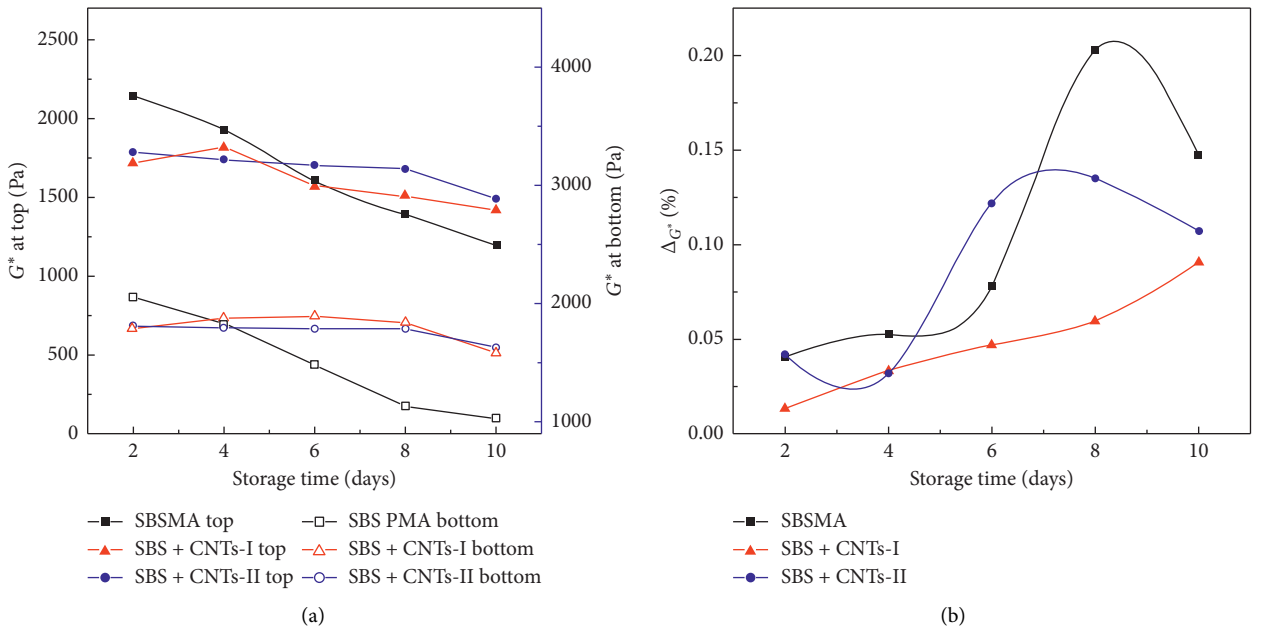

FIGURE 11: Difference in complex modulus ($G*$) and separation degree based on $G*$ ($\triangle G*$) of the three modified asphalts stored for 10 days. (a) $G*$ changes of asphalt samples. (b) $\triangle G*$ of asphalt samples.

fingerprint area (400–1000 cm^{-1}). In the functional group area, the observed wavenumbers at 2850, 2920, and 1450–1475 cm^{-1} demonstrated the existence of an aliphatic long chain in saturated hydrocarbon [18]. In the fingerprint area, SBS showed characteristic peaks at wavenumbers of 699, 760, 910, and 966 cm^{-1}, which belonged to benzene or aromatics [19]. The peaks at 699 and 966 cm^{-1} belonged to the polystyrene phase of SBS [20, 21]. The 966 cm^{-1}, which was the butadiene stretching vibration of SBS, has a stronger peak intensity of functional groups in SBS than 699 cm^{-1}. The base asphalt characteristic peaks included 1377, 1450–1475, 2850, and 2920 cm^{-1}. 1377 cm^{-1} represented the base asphalt [22]. The SBS characteristic peak index I_{SBS} was used in this study to capture the SBS amount changes in asphalt matrix, as shown in equation (2), where S_{966} and S_{1377} were the peak areas of 966 and 1377 cm^{-1}, respectively. The smaller the difference between the top and bottom I_{SBS} value, the better the thermal stability of modified asphalt.

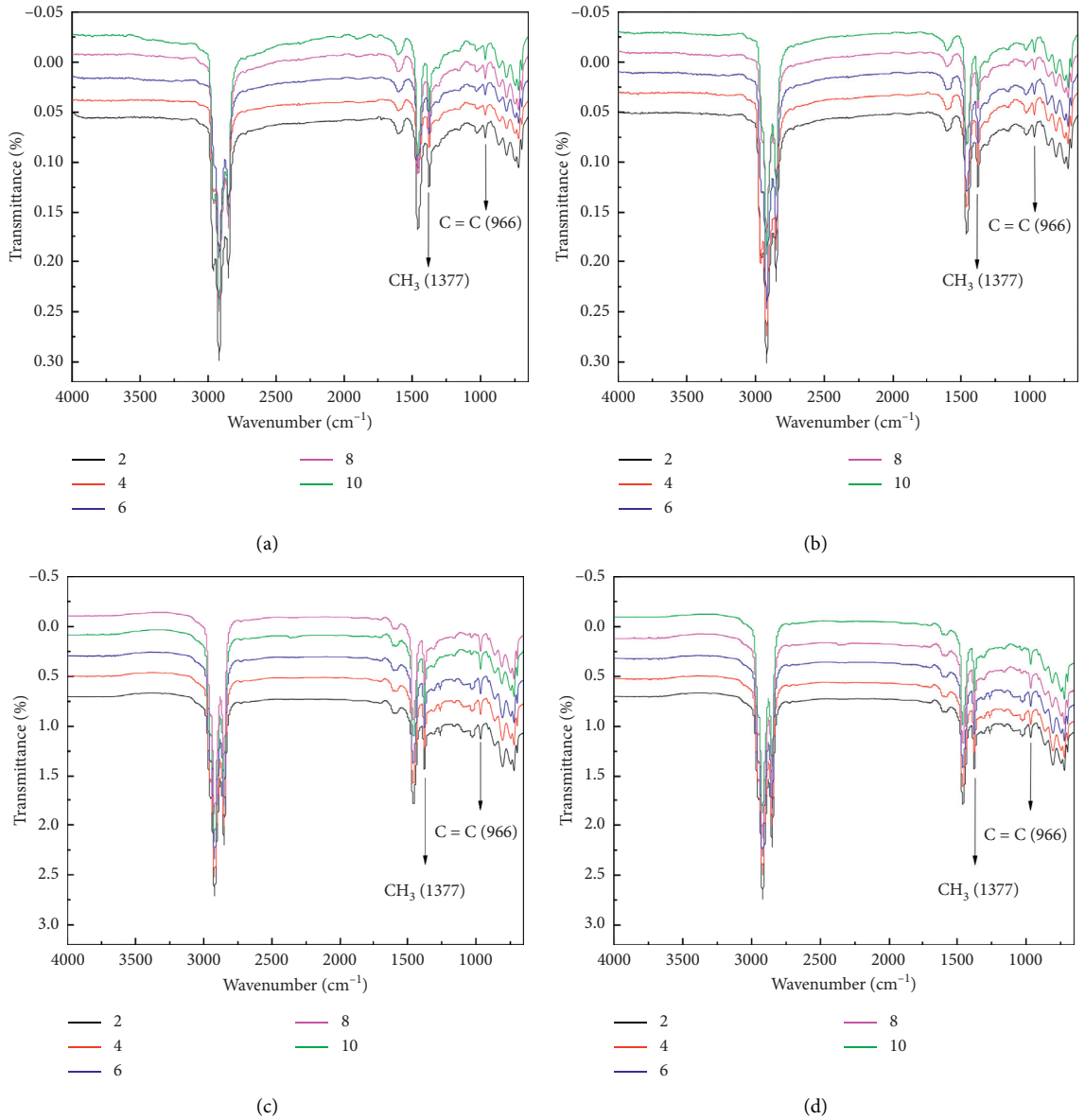

Figure 12: Continued.

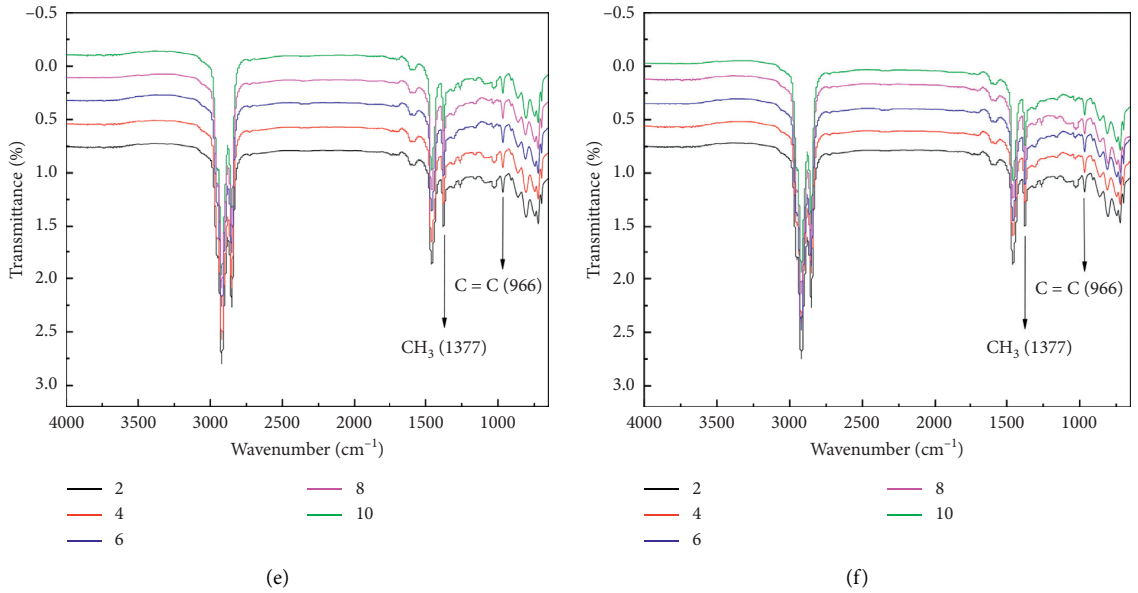

FIGURE 12: Infrared spectrum of three modified asphalts with different storage days. (a) The result of SBSMA at the top. (b) The result of SBSMA at the bottom. (c) The result of SBS + CNTs-I at the top. (d) The result of SBS + CNTs-I at the bottom. (e) The result of SBS + CNTs-II at the top. (f) The result of SBS + CNTs-II at the bottom.

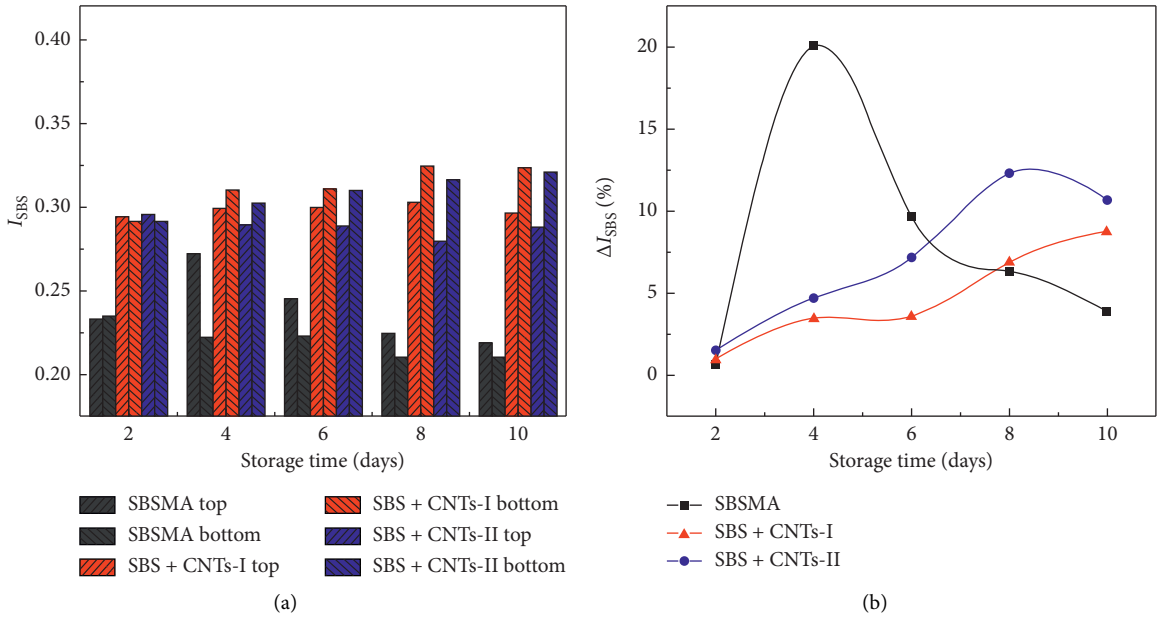

FIGURE 13: Characteristic peak area ratio separation and degree of three modified asphalts based on infrared spectra. (a) Changes of I_{SBS}. (b) Degree of separation based on I_{SBS}.

$$I_{SBS} = \frac{S_{966}}{S_{1377}} \times 100\%. \quad (2)$$

The results in Figure 12 showed that the peak strength of 1377 cm^{-1} for all samples either in the top or bottom changed with storage time due to base asphalt aging during the storage process. The peak changes at 1030 cm^{-1} prove the preceding finding. For the characteristic peaks of SBS, the peak strength at 966 cm^{-1} for SBSMA initially increased and then decreased at the top, while the values at the bottom decreased until storage time reached 10 days. For SBS + CNTs-I, the peak strength at 966 cm^{-1} at the top decreased with increasing storage time, while the values at the bottom slightly increased with storage time. This finding showed similar rules for SBS + CNTs-II, thus revealing different I_{SBS}.

Figure 13 provides the I_{SBS} and separation degree changes based on I_{SBS} in storage for 10 days. I_{SBS} of SBSMA at the top increased in the last 4 days and then decreased

until 10 days in Figure 13(a). A large I_{SBS} illustrated a large SBS amount in the asphalt. Thus, the rules demonstrated that SBS particles floated up with the increase in storage time. This phenomenon resulted in a large SBS content in the top but a small SBS amount in the bottom due to a smaller density for SBS than asphalt. The results also demonstrated that the phase separation mainly occurred within 4 days and remained stable in the last 6 days. The indexes of I_{SBS} for the samples with CNTs were slightly changed during 10 days of storage. Comparing the two types of CNTs, I_{SBS} of the samples with CNTs-I at the top revealed almost no changes with storage time, while the one with CNTs-II was slightly decreased. The index of ISBS for samples with CNTs-I or CNTs-II increased with storage time at the bottom. This phenomenon revealed that the increase in SBS amount at the top of all samples was reduced by adding CNTs, while the slightly increased values at the bottom of all samples proved that the network between CNTs and SBS was insufficiently strong. Moreover, the network structure formed by the mixture of CNTs and SBS would lead to an increase in polymer density and facilitate the easy settlement of SBS to the bottom [23].

However, $\triangle$ I_{SBS} indicated a different result. In Figure 13(b), the $\triangle$ISBS for the samples with CNTs increased with storage time, and the one with CNTs-II showed large values at every point. The particle size of CNTs-II was significantly larger than that of CNTs-I. Thus, an evident increase in polymer density of CNTs-II and SBS leads to the easier settlement of SBS particle to the bottom than that of CNTs-I. $\triangle$ I_{SBS} of SBSMA was completely different, which increased in the last four days and then decreased until 10 days. Although $\triangle$ I_{SBS} of SBSMA decreased on the 10th day, the performance of SBSMA had been seriously damaged. A crusting phenomenon was observed on the 10th day of the SBSMA, demonstrating that SBS polymer was completely destroyed after 10 days of high-temperature storage. Thus, the difference softening point only between the top and bottom was not fit to capture the phase separation of polymer-modified asphalt.

3.3.2. Distribution and Swelling Degree of SBS-Rich Phase from FM. FM was used to capture the SBS-rich phase distribution characteristics for SBSMA with CNTs as listed in Figure 14. The FM images revealed that the degree of SBS swelling was calculated on the basis of equation (3) using digital image technology, which was used to estimate the compatibility of polymer and asphalt indirectly, as proposed by Sengoz [24]. In the equation, A_{PRP} is the area of SBS-rich phases, and A_{total} is the total area of SBSMA in FM images. The original FM images were processed with MATLAB to convert them into binary images, which only contained two-pixel values (namely, 0 and 1), and then to binary black (asphaltene-rich phases) or white (SBS-rich phases). A_{PRP} and A_{total} are finally obtained [25]. The degree of SBS swelling is listed in Figure 15.

$$\text{Degree of SBS swelling} = \frac{A_{PRP}}{A_{Total}} \times 100\%. \quad (3)$$

Figure 14 shows that the SBS-rich phases are bright yellow, while asphaltene-rich phases and CNTs are almost black due to the absence of fluorescence. For SBSMA, the number of particles and the particle size in the top part all increased, while their behaviours were completely opposite in the bottom as shown in Figure 14(a). These results were verified by Figure 13(a). For the samples with CNTs, the SBS-rich phase showed a smaller size and denser network than that of SBSMA. For SBS + CNTs-I, the particle size of the SBS-rich phase was slightly larger on the 10th day than that of the 2nd day either on the top or bottom. Meanwhile, the bottom of SBS + CNTs-I on the 10th day showed a considerable amount of SBS particles than that at the top. The rule was the same as the results in Figures 10 and 11 from FT-IR. For SBS + CNTs-II, the SBS network was substantially denser than that with CNTs-I. Even on the 10th day, the large SBS particles were still less than those in the SBS + CNTs-I.

Figure 15 shows the degree of SBS swelling for three modified asphalts with increasing storage time. For SBS modified asphalt, the degree of SBS swelling at the top was increased, yet these values sharply decreased with increasing storage time. This result demonstrated that with the increase of storage time, SBS floats on the asphalt surface, and the amount of SBS dissolved in the top significantly increased while that in the bottom decreased, finally leading to phase separation or segregation of SBSMA. After 4 days of storage, the phase separation gradually stabilized, but a large amount of SBS floats up, resulting in some SBS slowly precipitating from the asphalt and crust on the surface with the passage of time. Thus, the content of SBS in the bottom slightly decreased in the last 6 days, as the results from FT-IR in Figure 13. A downward trend of the bottom in Figure 15(a) was due to the severe phase separation initially and then gradual gentleness with the increase in time. The samples with CNTs showed a substantially denser SBS network than that of neat SBSMA. For the SBS + CNTs-I, an upward trend either in the top or bottom was observed with increasing storage time in Figure 15(b), thereby providing improved compatibility between SBS and asphalt to avoid separation. Wang attributed this increase to the channelling effect of CNTs to transport small molecules in asphalt and improve the compatibility between SBS and asphalt [26]. The SBS + CNTs-II showed an upward trend in the bottom in Figure 15(c), but a downward trend was observed in the top with increasing storage time. Despite the poor compatibility of the top of SBS + CNTs-II, the data were still larger than that of SBSMA. Thus, the results showed that additional CNTs could improve the thermal storage stability of SBSMA. However, the results from FM images unclearly identified the difference between CNTs-I and CNTs-II. Therefore, the AFM was selected to clarify this issue.

3.3.3. Particle Characteristics of SBS-Rich Phase from AFM. The particle characteristics of the SBS-rich phase for SBSMA with CNTs during long-term storage were captured from AFM, as presented in Figures 14 and 15. In AFM images, the dispersed phase showed some tiny white dots mainly comprising the SBS-rich phase, while the continuous phase

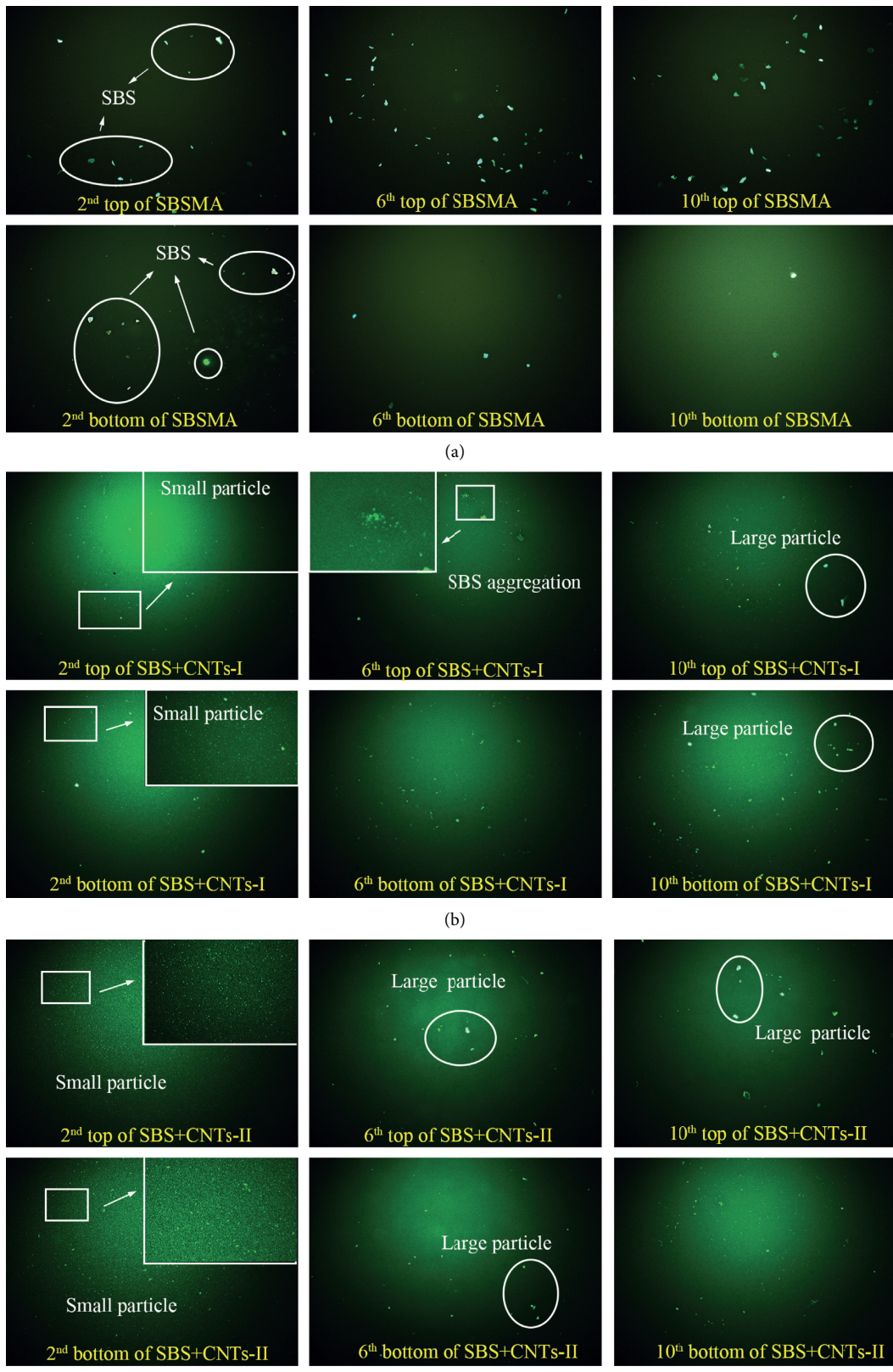

Figure 14: Fluorescence images of three modified asphalts with different storage times (magnification 100x). (a) FM images of SBS. (b) FM images of SBS + CNTs-I. (c) FM images of SBS + CNTs-II.

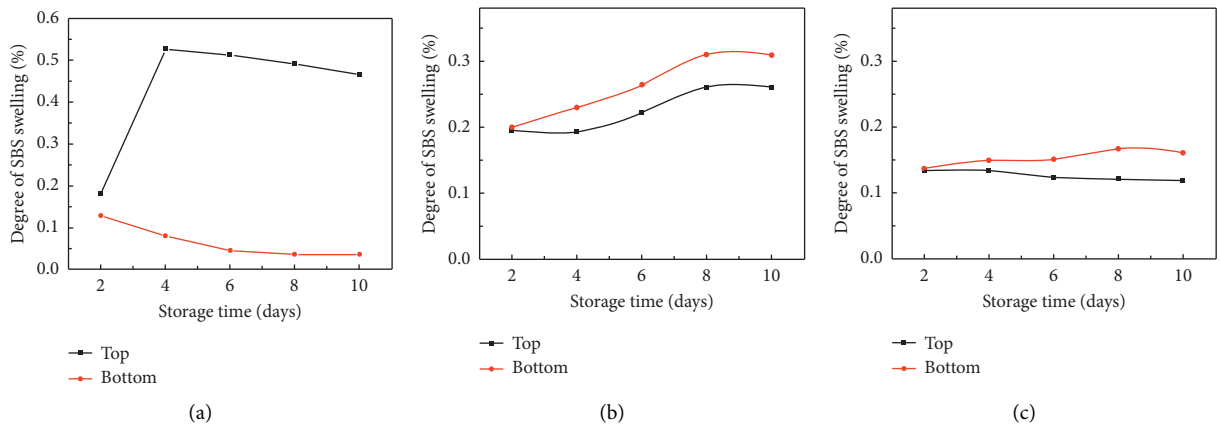

Figure 15: Degree of SBS swelling of three modified asphalt samples with different separation times. The samples of (a) SBSMA, (b) SBS + CNTs-I, and (c) SBS + CNTs-II.

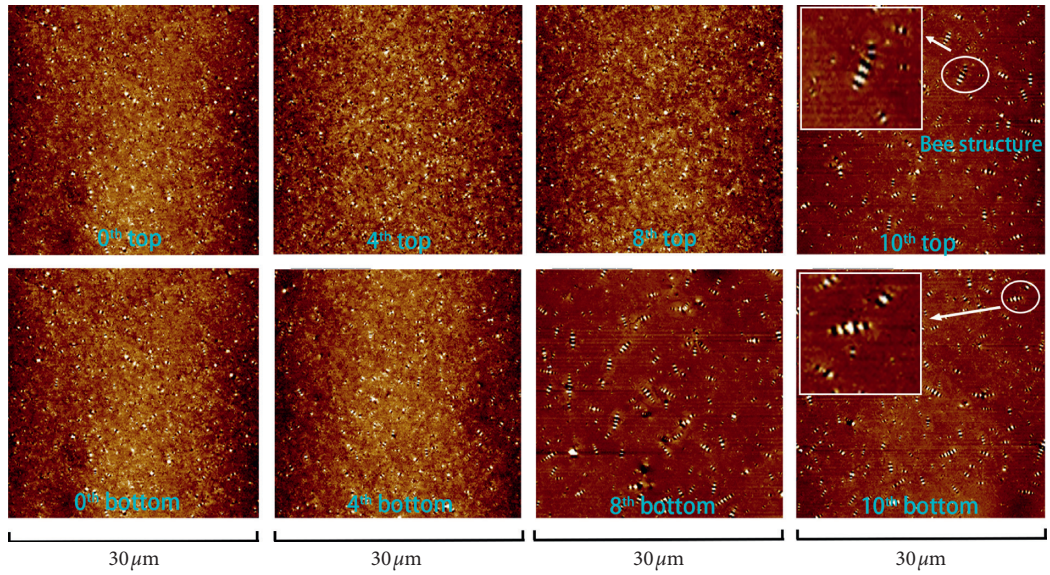

Figure 16: Phase diagram of SBS + CNTs-I with increasing storage time.

was the asphalt matrix. The bee structures of the base asphalt were ascribed to wax, asphaltene, and trace metals in asphalt [27, 28]. When adding SBS into asphalt, the bee structures were enclosed by swelled SBS, finally becoming blurred in AFM images [29]. Thus, the SBS-rich phase was used to identify the SBS network changes with increasing storage time.

For SBS + CNTs-I in Figure 16, determining the SBS-rich phases and asphalt matrix at the zero day is difficult, but the famous bee structure was still observed in the tiny white dots. After storage of 4 days, the size of the bee structure was slightly larger in the bottom than that in the top of SBS + CNTs-I. The images on the 8th day of SBS + CNTs-I revealed that the bee structure at the bottom was significantly larger than that at the top, thereby demonstrating the phase segregation occurrence. The images on the 10th day of SBS + CNTs-I indicated that the clear bee structure was observed at the top and bottom, thereby implying the degradation of SBS polymers. The bee structure size at the top was slightly larger than that at the bottom. For the sample of SBS + CNTs-II in Figure 17, the SBS-rich phase of SBS + CNTs-II at zero days was denser than that of SBS + CNTs-I. After storage of 10 days, the SBS network of SBS + CNTs-II at the top and bottom revealed insignificant deterioration. Thus, the surface roughness based on equations (4)–(6) from the nano scope analysis based on digital image technology was used for the quantitative description of the particle characteristics discrepancy. In the equation, R_q is the root mean square of roughness, R_a is the roughness average, $Z(x)$ is the function that describes the surface profile analysed considering height (Z) and position (x) of the sample over the evaluation length "L," and R_{max} is the maximum roughness.

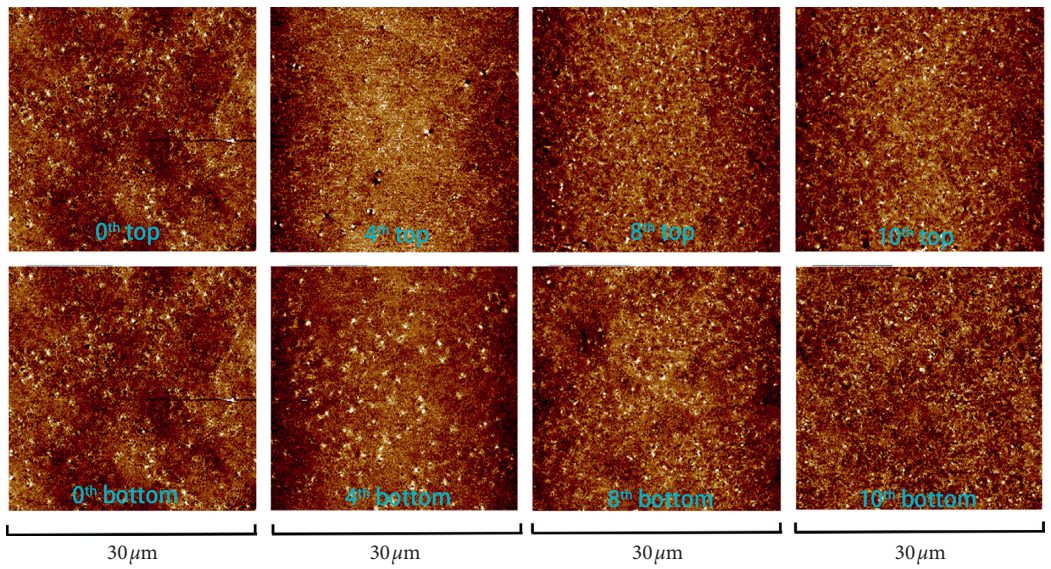

Figure 17: The phase diagram of SBS + CNTs-II with increasing storage time.

Table 4: The surface roughness of samples with different storage times.

Modifier	Storage time (days)	Top			Bottom		
		R_q	R_a	R_{max}	R_q	R_a	R_{max}
SBS + CNTs-I	0	1.41	1.05	36.2	1.41	1.05	36.2
	2	1.76	1.36	30.8	1.27	0.993	25.6
	4	1.16	0.859	33.0	1.44	1.10	27.1
	6	1.24	0.82	35.7	1.19	0.9	19.7
	8	1.09	0.796	39.3	2.46	1.19	87.6
	10	2.24	1.28	61.1	2.11	1.16	73.4
SBS + CNTs-II	0	1.03	0.751	40.7	1.03	0.751	40.7
	2	1.21	0.904	60.6	1.37	1.04	39.2
	4	1.26	0.984	32.8	1.20	0.911	30.8
	6	1.30	1.02	19.1	1.59	1.13	35.0
	8	1.30	0.997	29.5	1.20	0.916	18.5
	10	1.28	0.96	35.3	1.07	0.818	18.0

$$R_q = \left[\frac{1}{L}\int_0^L \left|Z^2(x)\right| dx\right]^{1/2}, \quad (4)$$

$$R_a = \frac{1}{L}\int_0^L |Z(x)|\, dx, \quad (5)$$

$$R_{max} = |\max Z(x)|. \quad (6)$$

Table 4 summarizes the surface roughness of asphalt samples with different storage times. For SBS + CNTs-I, R_q and R_a at the top with 2 days of storage were gradually increased due to base asphalt thermal aging and initial aggregation of small SBS particles to the large ones. In 2–4 days, the values of R_q and R_a started to decrease due to the absorption of some CNTs-I into SBS, easily sinking the large density of the dispersed phase to the bottom. In 4–8 days, the aggregation degree continued to worsen for SBS + CNTs-I. In 8–10 days, the aging for the base asphalt led to a crusting phenomenon and provided the largest R for the SBS + CNTs-I. For SBS + CNTs-II, R_q and R_a at the top slowly increased and slightly decreased. However, the increase in Rmax at the top was ascribed to the aggregation of the SBS-rich phase within 10 days. At the bottom of SBS + CNTs-II, although fluctuations in the values for R_q and R_a were observed, these fluctuations were small. Therefore, the overall situation was relatively stable. The overall trend of R_{max} slowed down, thereby illustrating that some SBS particles were still floating to the top part after 10 days of storage. Zhai et al. reported the polymer would entangle with carbon nanomaterials [30]. Thus, the phenomenon here would be ascribed to CNTs entangling with SBS. However, CNTs-II showed better inhibition effect on the aggregation of SBS particles than CNTs-I.

4. Conclusions

The elusive thermal storage stability of SBSMA has attracted wide attention for over half a century of intensive research. However, phase segregation constantly occurs after long-term thermal storage for SBSMA. Thus, this study aimed to investigate this issue using CNTs due to their excellent interface enhancement.

The role of CNT amount on the performance of SBSMA was investigated. The results revealed that SBSMA with different types of CNTs had different rules to the thermal storage stability. The optimum amount of CNTs for improving storage stability of SBSMA was 0.5 wt.%. This condition resulted in the smallest changes between the top and bottom for softening point difference, irrecoverable compliance, recovery rate, and complex modulus.

The macroperformance of SBSMA with CNTs within 10 days of storage was examined. The results revealed that for the difference of softening point, CNTs-II had no significant advantage in decreasing △SP of SBSMA but CNTs-I had. For rheological characteristics, after 10 days of storage, the largest R% of SBS modified asphalt (SBSMA) decreased to 2.24% and the smallest J_{nr} increased to 0.069 1/kPa, while R% of SBSMA with CNTs was 62.15% and its J_{nr} was 0.013 1/kPa. R% and J_{nr} of SBSMA with CNTs showed almost no change after 6 days of storage. Therefore, adding CNTs endowed the SBSMA with outstanding elastic recovery capability even after 10 days of storage. Moreover, adding CNTs slowed down the decay of complex modulus, and the CNTs-II showed better improvement than CNTs-I in SBSMA.

The microperformance of SBSMA with CNTs within 10 days storage was investigated by FT-IR, FM, and AFM. The results showed that SBS floated up in SBSMA but sank after adding CNTs. It was due to the entanglement between CNTs and SBS, which increases the density of SBS phase. Additional CNTs altered the distribution of SBS-rich phase and enhanced the swelling degree during the storage process. A small and dense network of SBS with CNTs was observed in FM and AFM images, thereby exhibiting improved thermal storage stability. Moreover, CNTs II worked better than CNTs I for improving storage stability of SBSMA; therefore, adding CNTs directly into SBSMA demonstrated less modification than the one premixed with SBS in advance. This study provided a new method to improve the thermal storage stability of polymer-modified asphalt.

Data Availability

The data used to support the findings of this study are included within the article.

Disclosure

This study was completed at the School of Transportation Engineering in Shandong Jianzhu University and at the School of Transportation Science and Engineering in Harbin Institute of Technology.

Conflicts of Interest

The authors declare that there are no conflicts of interest regarding the publication of this paper.

Acknowledgments

This research was funded by the National Natural Science Foundation of China (grant no. 51808322), Shandong Provincial Natural Science Foundation, China (grant no. ZR 2018B EE042), and Shandong University Youth Creation Team of China (grant no. 2019KJG004).

References

[1] A. Behnood and M. Modiri Gharehveran, "Morphology, rheology, and physical properties of polymer-modified asphalt binders," *European Polymer Journal*, vol. 112, pp. 766–791, 2019.

[2] W. Yin, F. Ye, and H. Lu, "Establishment and experimental verification of stability evaluation model for SBS modified asphalt: based on quantitative analysis of microstructure," *Construction and Building Materials*, vol. 131, no. 30, pp. 291–302, 2017.

[3] Í. A. de Carcer, R. M. Masegosa, M. Teresa Viñas et al., "Storage stability of SBS/sulfur modified bitumens at high temperature: influence of bitumen composition and structure," *Construction and Building Materials*, vol. 52, no. 15, pp. 245–252, 2014.

[4] G. Polacco, S. Filippi, F. Merusi, and G. Stastna, "A review of the fundamentals of polymer-modified asphalts: asphalt/polymer interactions and principles of compatibility," *Advances in Colloid and Interface Science*, vol. 224, pp. 72–112, 2015.

[5] X. Lu and U. Isacsson, "Compatibility and storage stability of styrene-butadiene-styrene copolymer modified bitumens," *Materials and Structures*, vol. 30, no. 10, pp. 618–626, 1997.

[6] D. Sun, F. Ye, F. Shi, and W. Lu, "Storage stability of SBS-modified road asphalt: preparation, morphology, and rheological properties," *Petroleum Science and Technology*, vol. 24, no. 9, pp. 1067–1077, 2007.

[7] V. Mouillet, J. Lamontagne, F. Durrieu, J.-P. Planche, and L. Lapalu, "Infrared microscopy investigation of oxidation and phase evolution in bitumen modified with polymers," *Fuel*, vol. 87, no. 7, pp. 1270–1280, 2008.

[8] T. Wang, X. Huang, and Y. Zhang, "Application of hansen solubility parameters to predict compatibility of SBS-modified bitumen," *Journal of Materials in Civil Engineering*, vol. 22, no. 8, 2010.

[9] D. Sun and W. Lu, "Investigation and improvement of storage stability of SBS modified asphalt," *Petroleum Science and Technology*, vol. 21, no. 5-6, pp. 901–910, 2003.

[10] D. Lesueur, "The colloidal structure of bitumen: consequences on the rheology and on the mechanisms of bitumen modification," *Advances in Colloid and Interface Science*, vol. 145, no. 1-2, pp. 42–82, 2009.

[11] J. Zhu, B. Birgisson, and N. Kringos, "Polymer modification of bitumen: advances and challenges," *European Polymer Journal*, vol. 54, pp. 18–38, 2014.

[12] T. Wang, T. Yi, and Z. Yuzhen, "The compatibility of SBS-modified asphalt," *Petroleum Science and Technology*, vol. 28, no. 7, pp. 764–772, 2010.

[13] J. Zhu, X. Lu, R. Balieu, and N. Kringos, "Modelling and numerical simulation of phase separation in polymer modified bitumen by phase-field method," *Materials & Design*, vol. 107, no. 5, pp. 322–332, 2016.

[14] E. Santagata, O. Baglieri, L. Tsantilis, and D. Dalmazzo, "Rheological characterization of bituminous binders modified with carbon nanotubes," *Procedia-Social and Behavioral Sciences*, vol. 53, no. 3, pp. 546–555, 2012.

[15] A. Goli, H. Ziari, and A. Amini, "Influence of carbon nanotubes on performance properties and storage stability of SBS modified asphalt binders," *Journal of Materials in Civil Engineering*, vol. 29, no. 8, 2017.

[16] J.-F. Masson, P. Collins, G. Robertson, J. R. Woods, and J. Margeson, "Thermodynamics, phase diagrams, and stability of Bitumen–Polymer blends," *Energy & Fuels*, vol. 17, no. 3, pp. 714–724, 2003.

[17] S. Aflaki and P. Hajikarimi, "Implementing viscoelastic rheological methods to evaluate low temperature

performance of modified asphalt binders," *Construction and Building Materials*, vol. 36, pp. 110–118, 2012.

[18] D. Zhang, H. Zhang, C. Zhu, and C. Shi, "Synergetic effect of multi-dimensional nanomaterials for anti-aging properties of SBS modified bitumen," *Construction and Building Materials*, vol. 144, no. 30, pp. 423–431, 2017.

[19] F. Zhang, J. Yu, and J. Han, "Effects of thermal oxidative ageing on dynamic viscosity, TG/DTG, DTA and FTIR of SBS- and SBS/sulfur-modified asphalts," *Construction and Building Materials*, vol. 25, no. 1, pp. 129–137, 2011.

[20] A. C. Falchetto and K. H. Moon, "Micromechanical-analogical modelling of asphalt binder and asphalt mixture creep stiffness properties at low temperature," *Road Materials and Pavement Design*, vol. 16, no. 1, pp. 111–137, 2015.

[21] H.-l. Zhang, M.-m. Su, S.-f. Zhao, Y.-p. Zhang, and Z.-p. Zhang, "High and low temperature properties of nano-particles/polymer modified asphalt," *Construction and Building Materials*, vol. 114, no. 1, pp. 323–332, 2016.

[22] C. Yan, W. Huang, J. Ma et al., "Characterizing the SBS polymer degradation within high content polymer modified asphalt using ATR-FTIR," *Construction and Building Materials*, vol. 233, no. 10, Article ID 117708, 2020.

[23] V. Mouillet, F. Farcas, and E. Chailleux, "Physico-chemical techniques for analysing the ageing of polymer modified bitumen," *Polymer Modified Bitumen*, pp. 366–395, 2011.

[24] G. Polacco, J. Stastna, D. Biondi, and L. Zanzotto, "Relation between polymer architecture and nonlinear viscoelastic behavior of modified asphalts," *Current Opinion in Colloid & Interface Science*, vol. 11, no. 4, pp. 230–245, 2006.

[25] S. M. Asgharzadeh, N. Tabatabaee, K. Naderi, and M. N. Partl, "Evaluation of rheological master curve models for bituminous binders," *Materials and Structures*, vol. 48, no. 1-2, pp. 393–406, 2015.

[26] P. Wang, F. Zhai, Z.-j. Dong, L.-z. Wang, J.-p. Liao, and G.-r. Li, "Micromorphology of asphalt modified by polymer and carbon nanotubes through molecular dynamics simulation and experiments: role of strengthened interfacial interactions," *Energy & Fuels*, vol. 32, no. 2, pp. 1179–1187, 2018.

[27] A. T. Pauli, R. W. Grimes, A. G. Beemer, T. F. Turner, and J. F. Branthaver, "Morphology of asphalts, asphalt fractions and model wax-doped asphalts studied by atomic force microscopy," *International Journal of Pavement Engineering*, vol. 12, no. 4, pp. 291–309, 2011.

[28] Å. L. Lyne, V. Wallqvist, and B. Birgisson, "Adhesive surface characteristics of bitumen binders investigated by atomic force microscopy," *Fuel*, vol. 113, pp. 248–256, 2013.

[29] L. Loeber, G. Muller, J. Morel, and O. Sutton, "Bitumen in colloid science: a chemical, structural and rheological approach," *Fuel*, vol. 77, no. 13, pp. 1443–1450, 1998.

[30] F. Zhai, Y. Feng, K. Zhou, L. Wang, Z. Zheng, and W. Feng, "Graphene-based chiral liquid crystal materials for optical applications," *Journal of Materials Chemistry C*, vol. 7, no. 8, pp. 2146–2171, 2019.